Inorg. Chem. **2008**, *47*, 4734−4739

Inorganic Chemistry

Article

Charge, Orbital, and Magnetic Ordering in $YBaFe_2O_5$ from First-Principles Calculations

Xianfeng Hao,[†,‡] Yuanhui Xu,[§] Minfeng Lv,[†] Defeng Zhou,[§] Zhijian Wu,[†] and Jian Meng*[,†]

Key Laboratory of Rare Earth Chemistry and Physics, Changchun Institute of Applied Chemistry, Chinese Academy of Sciences, Changchun 130022, P.R. China, School of Biological Engineering, Changchun University of Technology, Changchun 130012, P.R. China, and Graduate School, Chinese Academy of Sciences, Beijing 100049, P.R. China

Received January 13, 2008

First principles calculations using the augmented plane wave plus local orbitals method, as implemented in the WIEN2k code, have been used to investigate the electronic and magnetic properties of $YBaFe_2O_5$, especially as regards the charge-orbital ordering. Although the total 3d charge disproportion is rather small, an orbital order parameter defined as the difference between t_{2g} orbital occupations of Fe^{2+} and Fe^{3+} cations is large (0.73) and gives unambiguous evidence for charge and orbital ordering. Strong hybridization between O 2p and Fe e_g states results in the nearly complete loss of the separation between the total charges at the Fe^{2+} and Fe^{3+} atoms. Furthermore, the relationship between the orbital ordering and charge ordering is also discussed. The d_{xz} orbital ordering is responsible for the stability of the G-type antiferromagnetic spin ordering and the charge ordering pattern.

Introduction

In recent years there has been an upsurge of interest in perovskite-like transition metal oxides as a result of the wide range of physical properties that they exhibit. The physical properties, such as electronic transport and magnetism, of transition metal oxides are intimately related to charge and orbital ordering.[1–5] The compounds exhibit charge and orbital orderings which manifest themselves in the spatial localization of the charge carriers on certain ionic sites and in the real space ordering of the charge carriers, in particular, electronic orbitals, respectively. Because the magnetic ordering is sensitive to the changes in the filling of the d orbitals, charge ordering transitions should in principle be strongly coupled with both orbital and magnetic transitions. Furthermore, it is well established in the early works of Goodenough and Kanamori[6] that the superexchange interaction between neighboring transition metal ions is strongly dependent on the spatial orientation of occupied d orbitals leading to even sign changes in this interaction for different orbital occupations in orbitally ordered materials as discussed by Khomskii and Kugel.[7] Therefore, the fundamental mechanisms that give rise to charge and orbital ordering are of considerable current interest.

One of the classical examples of mixed valent system is $YBaFe_2O_5$,[8] which adopts an oxygen-deficient perovskite-type structure containing double layers of corner sharing FeO_5 square pyramids separated by Y^{3+} ions. At high temperatures, tetragonal (*P*4/*mmm*) $YBaFe_2O_5$ is a fractional valent material with the Fe atoms possessing a normal valence of 2.5+ and paramagnetism. On cooling, the compound orders antiferromagnetically at $T_N = 425$ K but remains valence mixed. The magnetic structure is characterized by antiferromagnetic (AFM) Fe−O−Fe superexchange coupling within the double layers and a ferromagnetic (FM) Fe−Fe direct exchange coupling between neighboring double

---

* To whom correspondence should be addressed. E-mail: jmeng@ciac.jl.cn. Fax: +86-431-85698041.

[†] Changchun Institute of Applied Chemistry, Chinese Academy of Sciences.

[‡] Graduate School, Chinese Academy of Sciences.

[§] Changchun University of Technology.

(1) Radaelli, P. G.; Cox, D. E.; Marezio, M.; Cheong, S. -W. *Phys. Rev. B* **1997**, *55*, 3015.
(2) Jeng, H. -T.; Guo, G. Y.; Huang, D. J. *Phys. Rev. B* **2006**, *74*, 195115.
(3) Goodenough, J. B. *Phys. Rev.* **1955**, *100*, 564.
(4) Wollan, E. O.; Koehler, W. C. *Phys. Rev.* **1955**, *100*, 545.
(5) Popović, Z.; Satpathy, S. *Phys. Rev. Lett.* **2002**, *88*, 197201.
(6) (a) Goodenough, J. B. *Magnetism and the Chemical Bond*; Interscience Publisher: New York, 1963. (b) Kanamori, J. *J. Phys. Chem. Solids* **1959**, *10*, 87.
(7) Kugel, K. I.; Khomskii, D. I. *Sov. Phys. JETP* **1973**, *37*, 725.
(8) Woodward, P. M.; Karen, P. *Inorg. Chem.* **2003**, *42*, 1121.

10.1021/ic800060c CCC: $40.75

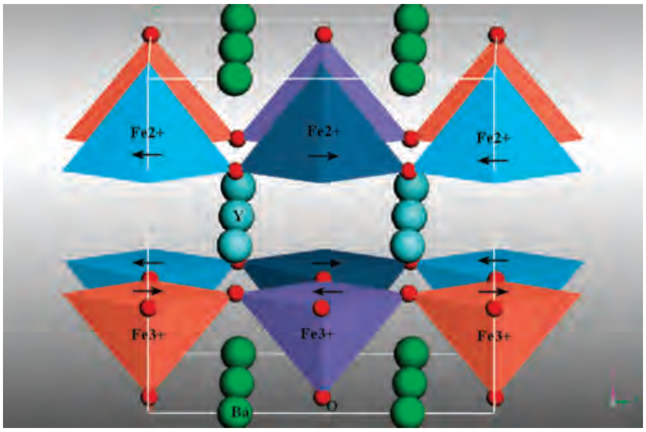

Figure 1. Crystal and magnetic (G-type) structure for $YBaFe_2O_5$.

layers. At $T_V = 308$ K, a Verwey-type transition orders the Fe valences in real space and also triggers a number of changes in the crystal and the AFM structure (Figure 1).[8] The crystal structure rearranges to accommodate alternating chains of Fe^{2+} and Fe^{3+} running along the *b* axis and exhibits orthorhombic features (*Pmma*); at the same time, the magnetic structure accommodates to a G-type AFM configuration, where both the Fe−O−Fe superexchange and the Fe−Fe direct exchange coupling are AFM (Figure 1). Apparently, the main difference between these two magnetic structures is the sign of the direct exchange interaction between doubling layers (across the Y layer). More interestingly, the unexpectedly large cooperative Jahn–Teller distortion for the Fe^{2+} ions induces an ordering of the doubly occupied d_{xz} orbitals.

However, despite intensive investigations of the charge-orbital ordering phenomena,[1–5] the detailed pattern or even the existence of the charge ordering in $YBaFe_2O_5$, or in general, the relationship between charge-orbital ordering and spin ordering is still not fully resolved. Thus, theoretical calculations based on density-functional theory (DFT) that can provide further details about the structural, electronic, and magnetic properties of $YBaFe_2O_5$ and related physical properties therefore are highly desirable, especially as regards the orbital ordering.

Approach

All calculations reported in this work were carried out using the highly accurate full-potential linearized augmented plane wave plus local orbitals (FP-LAPW+lo) method[9,10] with DFT, implemented in the WIEN2k package.[11,12] In this method, the space is divided into an interstitial region (IR) and nonoverlapping muffin-tin (MT) spheres centered at the atomic sites. In the MT region, the basis sets are described by radial solutions of the one-particle Schrödinger equation (at fixed energy) and their energy derivatives are multiplied by spherical harmonics.

To achieve energy convergence, the wave functions in the interstitial region were expanded in plane waves with a cutoff $R_{MT}^{min}K_{max} = 7$, where R_{MT}^{min} denotes the smallest atomic sphere radius and K_{max} gives the magnitude of the largest *K* vector in the plane-wave expansion. The values of the atomic sphere radii (R_{MT}) were chosen as 2.35, 2.5, 1.86, and 1.65 a.u for Y, Ba, Fe, and O, respectively. The valence wave functions inside the spheres are expanded up to $l_{max} = 10$, while the charge density was Fourier expanded up to $G_{max} = 14$. The total Brillouin zone was sampled with 1000 *k* points. The Brillouin zone integration is carried out with a modified tetrahedron method.[13] Self-consistency is considered to be achieved when the total-energy difference between succeeding iterations is less than 10^{-5} Ry per formula unit.

As for the exchange-correlation potential, we employed the standard generalized gradient approximation (GGA) using the PBE scheme.[14] In addition, to properly describe the strong electron correlation in the 3d transition-metal oxides, the GGA plus on site repulsion *U* method (GGA+*U*) was used[15–17] with the effective *U* values ($U_{eff} = U - J$) of 1.0–5.0 eV. In our calculations, we have adopted the experimental structure data reported in ref 2 and displayed in Figure 1.

Results and Discussion

To gain insight into the electronic and magnetic properties in the orthorhombic form of $YBaFe_2O_5$, the nonmagnetic (NM) state was calculated by performing nonspin-polarized electronic structure calculations via enforced spin degeneracy for all species. Our calculations indicate the charge transfer from the cations to the anionic sites of oxygen, but the amount of charge transfer is smaller than that of an ionic character of the atomic constituents. The total density of states (TDOS) for the NM state is presented in Figure 2a. The large DOS at the Fermi level suggests that this state is metallic. Furthermore, the Fermi level occurs near the DOS peak dominated by Fe 3d states. Within the Stoner theory,[18] the large DOS at the Fermi level is related to the instability of the NM configuration with respect to the onset of intraband spin polarization when $n(E_F)I > 1$. In this so-called Stoner criterion I is the Stoner integral: $I(\mathrm{Fe}) = 0.42$ eV for an fcc structure.[19] With $n_{\mathrm{Fe}}(E_F) = 5.80\ \mathrm{eV}^{-1}$, the resultant $n(E_F)I$ value of 2.44 unambiguously points to an instability toward spin polarization. Indeed, the further spin-polarized calculations (see below) confirmed this statement.

---

(9) Sjöstedt, E.; Nordström, L.; Singh, D. J. *Solid State Commun.* **2000**, *114*, 15.

(10) Madsen, G. K. H.; Blaha, P.; Schwarz, K.; Sjöstedt, E.; Nordström, L. *Phys. Rev. B* **2001**, *64*, 195134.

(11) Schwarz, K.; Blaha, P. *Comput. Mater. Sci.* **2003**, *28*, 259.

(12) Blaha, P.; Schwarz, K.; Madsen, G. K. H.; Kvasnicka, D.; Luitz, J. *WIEN2k, An Augmented Plane Wave Plus Local Orbitals Program for Calculating Crystal Properties*; Vienna University of Technology: Austria, 2001; ISBN 3-9501031-1-2.

(13) Blöchl, P. E. *Phys. Rev. B* **1994**, *50*, 17953.

(14) Perdew, J.; Burke, S.; Ernzerhof, M. *Phys. Rev. Lett.* **1996**, *77*, 3865.

(15) Lichtenstein, A.; Anisimov, V.; Zaanen, J. *Phys. Rev. B* **1995**, *52*, R5467.

(16) Anisimov, V.; Aryasetiawan, F.; Lichtenstein, A. *J. Phys.: Condens. Matter* **1997**, *9*, 767.

(17) Petukhov, A.; Mazin, I.; Chioncel, L.; Lichtenstein, A. *Phys. Rev. B* **2003**, *67*, 153106.

(18) Sahnoun, M.; Daul, C.; Haas, O.; Wokaun, A. *J. Phys.: Condens. Matter* **2003**, *17*, 7995.

(19) Sigalas, M. M.; Papaconstantopoulos, D. A. *Phys. Rev. B* **1994**, *50*, 7255.

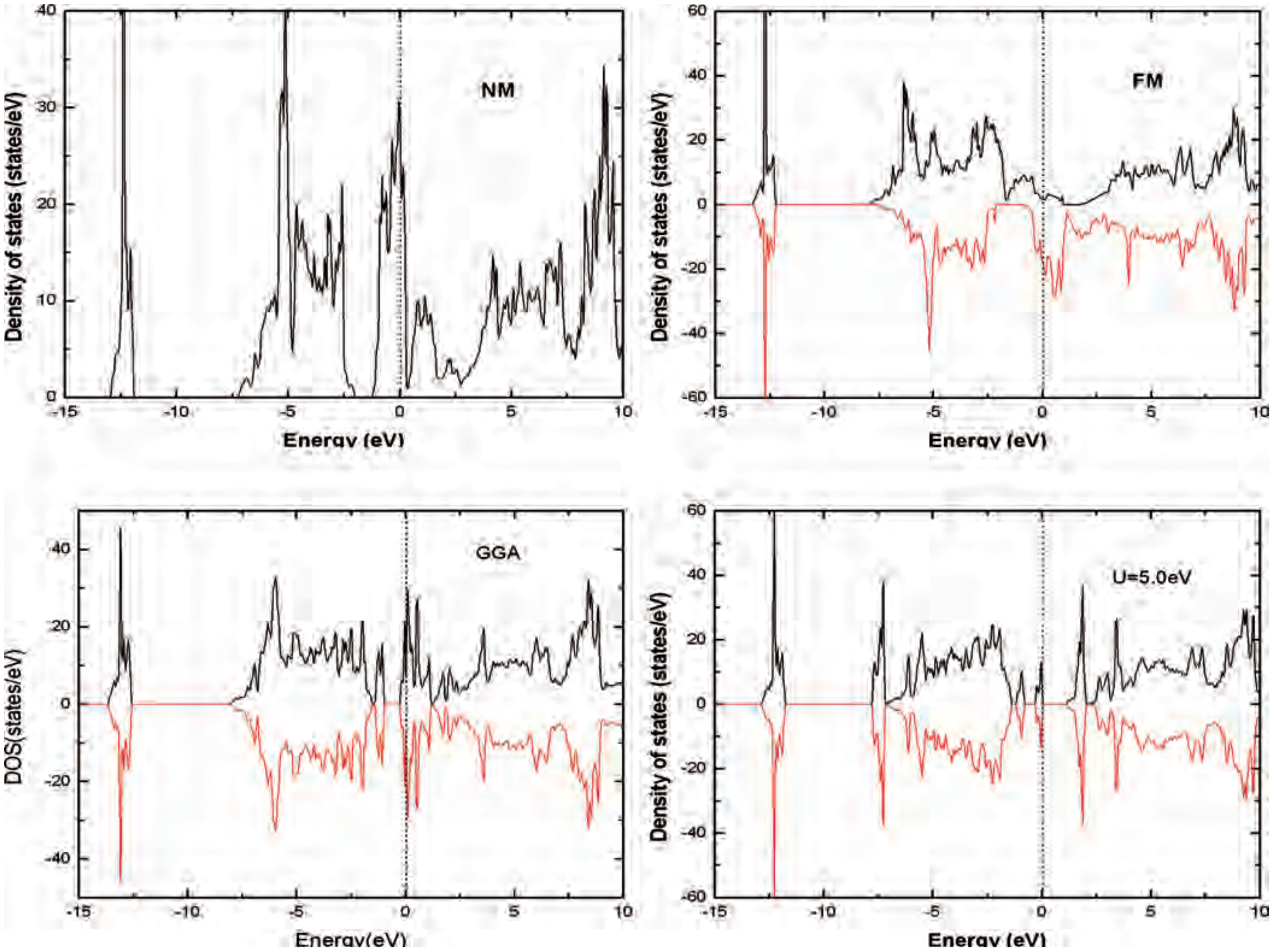

Figure 2. Calculated total densities of states of the NM, FM, G-type AFM $U = 0.0$ eV and $U = 5.0$ eV structures of $YBaFe_2O_5$, respectively. The Fermi level is set to zero. Majority and minority spins are shown above and below the axes, respectively.

Spin-polarized electronic structure calculations were performed for the FM configuration, and its TDOS is displayed in Figure 2b. The majority and minority spins are shown above and below the axes. For the FM ordering, the electronic structure is found to be metallic with near Fermi level DOS dominated by the Fe^{2+} 3d states. The total energy obtained for the FM configuration is by 1.64 eV/f.u. lower than that of the NM state, which is consistent with the finding that the $YBaFe_2O_5$ is apt to possess a nonzero magnetic moment on the Fe sites. The calculated local magnetic moments are 3.25–3.30 μ_B and 0.15–0.27 μ_B for Fe and O, respectively. The failure of a distinction between Fe^{2+} and Fe^{3+} from the theoretical magnetic moments is associated with the metallic character for the FM state. The local magnetic moments of the Fe^{2+} and Fe^{3+} ions are largely reduced from the high spin d^6 and d^5 configurations (formally 4 and 5 μ_B), respectively. The reduction of local magnetic moments of Fe and the finite magnetic moments of O atoms originate from the strong hybridization of the Fe−O bonds. However, the FM configuration is not the magnetic ground-state of $YBaFe_2O_5$.[8,20] We, therefore, carried out G-type calculations on the AFM state observed experimentally (the AFM interaction in three directions, Figure 1), as will be discussed below. Note that the NM and FM configurations (they are experimentally inaccessible) just provide useful references to understand the G-type AFM configuration observed in experiment.

Our total energy obtained for the G-type AFM configuration shows that it is considerably more stable than the FM state (0.73 eV per formula), which is in good agreement with the neutron powder diffraction (NPD). In the remainder of this work we will consider only the results calculated for the G-type AFM state.

The TDOS of $YBaFe_2O_5$ in the G-type configuration is shown in Figure 2c obtained by the GGA scheme. The GGA calculation gives a metallic ground-state with finite states at the Fermi level (E_F) being inconsistent with the expectation: it is an insulator. This expectation is related to the finding that $YBaFe_2O_5$ exhibits a charge-orbital ordering feature below the Verwey-type transition temperature 308 K.[8] The incorrect description of the electronic properties could be due to the well-known inefficiency of pure DFT in describing systems with strong intra-atomic interaction (or on-site Coulomb repulsion U and exchange interaction J), and it is

---

(20) Chang, S.; Karen, P.; Hehlen, M. P.; Trouw, F. R.; McQueeney, R. J. *Phys. Rev. Lett.* **2007**, *99*, 037202.

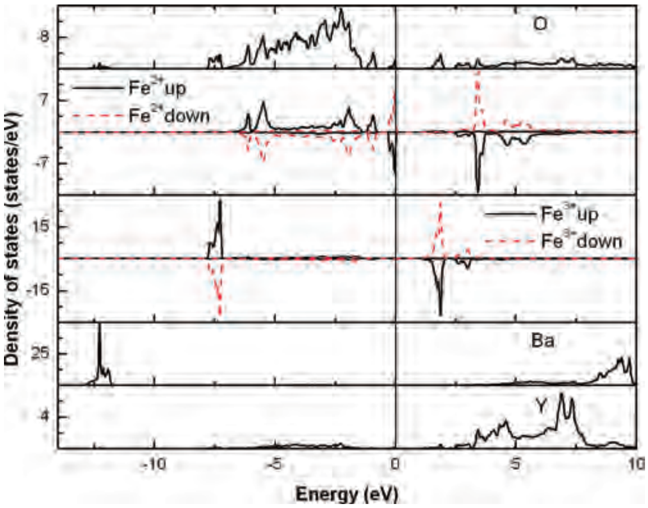

Figure 3. Site-decomposed electronic DOS for a G-type AFM configuration for orthorhombic $YBaFe_2O_5$ obtained by GGA+U within $U = 5.0$ eV.

necessary to overcome this problem for transition metal oxides.

Following the procedure of Anisimov et al.[15,16] in which the strong intra-atomic interaction depends only on the difference of U and J, that is, the effective value U_{eff}, we apply a constant term of 5.0 eV to the density functional, as it was adopted for Fe_3O_4,[21] $LuFe_2O_4$,[22] and related other iron oxides.[23] As can be seen from Figure 2d, an insulating band structure is obtained with a finite band gap. In the previous studies of related iron oxides, various values in the range 1.0–5.0 eV have been adopted for the on-site Coulomb and exchange term.[21–23] The general good agreement with experimental observations indicates that 5.0 eV is a reasonable value. However, to ensure that the calculated electronic and magnetic properties of $YBaFe_2O_5$ are reliable, we examined the effective value U_{eff} dependence of the insulating behavior. The energy gap between the occupied and unoccupied states increases considerably from 0.1 eV for $U_{\mathrm{eff}} = 1.0$ eV up to 1.20 eV for $U_{\mathrm{eff}} = 5.0$ eV. This remarkable increase in the gap value is accompanied by the enhancement of the spin magnetic moment from 3.36 up to 3.96 μ_B for the Fe^{3+} cation and from 2.99 up to 3.37 μ_B for the Fe^{2+} cation as U_{eff} increases from 0.0 to 5.0 eV.

The spin and site decomposed DOS for the G-type AFM state obtained by GGA+U within $U = 5.0$ eV is presented in Figure 3. The DOS contribution from Y and Ba is negligibly small indicating a high degree of ionic bonding between them and the host lattice. The main valence band consists of both oxygen p states and iron d states while the conduction band is dominated by iron d states, with partial contribution from Y p states. Because of the charge ordering, the Fe atoms split into subgroups of 2+ and 3+ Fe cations with equal numbers. Thus, for the G-type AFM configuration, one of t_{2g} majority/minority spin states of the Fe^{2+} atoms becomes completely occupied, whereas all other t_{2g} bands are pushed by the strong Coulomb interaction to the energies above 3 eV. On the other hand, the majority/minority spin 3d states of Fe^{3+} atoms are shifted below the O 2p states, which form the band in the energy range from −8 to −2 eV. In contrast to the Fe^{3+} states, the 3d states of Fe^{2+} form the broad bands between −7 eV to the Fermi level. The energy gap is opened between occupied and unoccupied t_{2g} states of Fe^{2+} and Fe^{3+}, respectively. As a consequence, the calculated magnetic moments of Fe^{2+} and Fe^{3+} are 3.37 μ_B and 3.96 μ_B in accord with the high spin state of the d^6 and d^5 electronic configurations, respectively.

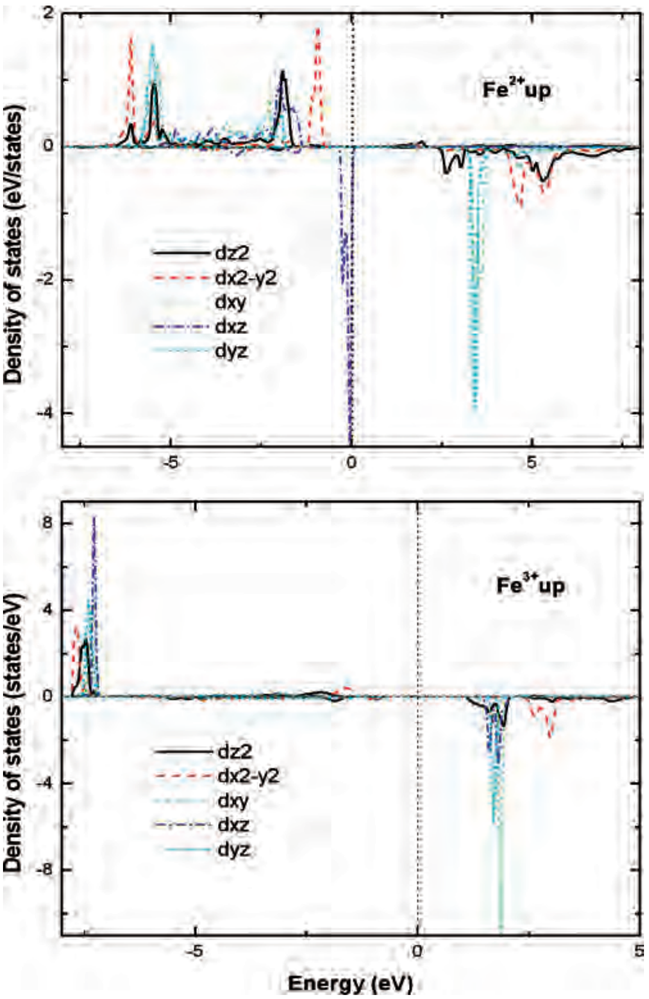

Figure 4. Orbital-decomposed electric DOS (d orbital only) of Fe^{2+} and Fe^{3+} (spin up) in the G-type AFM ground configuration obtained by GGA+U within $U = 5.0$ eV. Because of the AFM structure, there are another kind of Fe^{2+} and Fe^{3+} ions, i.e., Fe^{2+} and Fe^{3+} (spin down); their distribution of spin up and down states are completely opposite to that of Fe^{2+} and Fe^{3+} (spin up). To simplify, this is not shown in the figure.

As is fair typical, the calculated difference of magnetic moments (0.59 μ_B), the corresponding total 3d charge differences (0.26e), and the disproportion of the total electron charges insides the atomic spheres of the Fe^{2+} and Fe^{3+} cations (0.17e) are small. Because of the strong screening effects of the O 2p−Fe 3d e_g σ-type bonds, the nature of the charge ordering is partially enshrouded. Intriguingly, an analysis of the occupation matrices of the 3d Fe^{2+}/Fe^{3+} states in detail confirms the substantial charge separation. As shown in Figure 4, it is utterly evident that one of the $t_{2g}\downarrow$ states of

---

(21) Leonov, I.; Yaresko, A. N.; Antonov, V. N.; Anisimov, V. I. *Phys. Rev. B* **2006**, *74*, 165117.

(22) Xiang, H. J.; Whangbo, M.-H. *Phys. Rev. Lett.* **2007**, *98*, 246403.

(23) Leonov, I.; Yaresko, A. N.; Antonov, V. N.; Attfield, J. P.; Anisimov, V. I. *Phys. Rev. B* **2005**, *72*, 014407.

the Fe^{2+} cations is almost completely filled with the integrated occupation number $n \approx 0.84$; on the other hand, the occupation numbers of the $t_{2g}\downarrow$ orbitals for the Fe^{3+} ions have negligible population (do not exceed 0.11). According to the definition by Leonov et al.,[21,23–25] the well-defined order parameter is the difference of the t_{2g} populations for the Fe^{2+} and Fe^{3+} cations, which gives the value of about 73% of the ideal ionic charge ordering and clearly demonstrates the existence of charge ordering below the Verwey-type transition. The valence separation is considerably larger than in the classical charge ordering, though not fully understood, for example, in magnetite[25] and in the colossal magnetoresistance manganites,[26] whereas it is significantly smaller than in Fe_2OBO_3.[27]

Remarkably, our self-consistent field calculations obtained from the GGA+U approach is not only charge but also orbitally ordered. This is illustrated in Figure 4 which shows the orbital-decomposed electric DOS (d orbital only) of Fe^{2+} and Fe^{3+}. The first point that should be underlined is the crystal-field splitting in the square-pyramidal coordination. It is clear that the d_{xy}, d_{xz}, and d_{yz} orbitals are nearly degenerate in energy, while the d_{z^2} orbital lies somewhat higher and the $d_{x^2-y^2}$ orbital sites are substantially higher in energy. This crystal-field splitting is excellently consistent with those pattern obtained from the extended Hückel calculations.[8] More importantly, the $t_{2g}\downarrow$ band of the two Fe^{2+} ions are of predominated d_{xz} orbital characters, with the other two orbitals nearly unoccupied. These results unambiguously indicate the formation of orbital ordering in the Fe^{2+} ions of $YBaFe_2O_5$. To visualize the orbital ordering pattern in detail, we illustrate the isosurface of the spin density (0.15e/Å^3) corresponding to the $t_{2g}\downarrow$ band of Fe^{2+} ions just below the Fermi level (Figure 5). From the obtained orbital ordering pattern it is clearly seen that there exists a d_{xz} character in the crystal coordinates. Because all the Fe^{2+} ions are antiferromagnetically coupled along the *b* axis in the G-type AFM state, the obtained orbital order is consistent with the ferro-orbital AFM state, which is consistent with the Kugel−Khomskii theory.[7] Furthermore, the orientation of the occupied Fe^{2+} $t_{2g}\downarrow$ orbitals is consistent with the large average Fe−O distance in the *xz* plane. According to the experiment,[8] the Fe−O_{ax} distance (2.052 Å) and the Fe^{2+}−O_{eq} distance (2.109 Å) in the *xz* plane are considerably larger than the average bond distance of Fe−O_{eq} (1.959 Å) in the *yz* plane (where the subscripts O_{ax} and O_{eq} refer to axial and equatorial, respectively). These results suggested that the cooperative Jahn–Teller distortion in turn favors the orbital ordering.

As mentioned above, the superexchange interaction between neighboring transition metal ions is strongly dependent on the spatial orientation of the occupied d orbitals. On the basis of the so-called Goodenough−Kanamori−Anderson (GKA) rules, the consideration of the orbital population in insulating $YBaFe_2O_5$ results in the G-type AFM state. In sharp contrast to the AFM coupling cross the oxygen-defect Y layers below the Verwey transition, the phase above exhibits FM interaction across the oxygen-defect Y layers.[8] The rationale for this variation was the argument that the FM exchange is stabilized by the metallic character of the compound above the transition, which is validated by further calculation for this phase. On cooling, the charge-orbital ordering occurs, the d electrons will be localized, and the superexchange mechanism stabilizing the AFM insulating ground-state is enhanced.

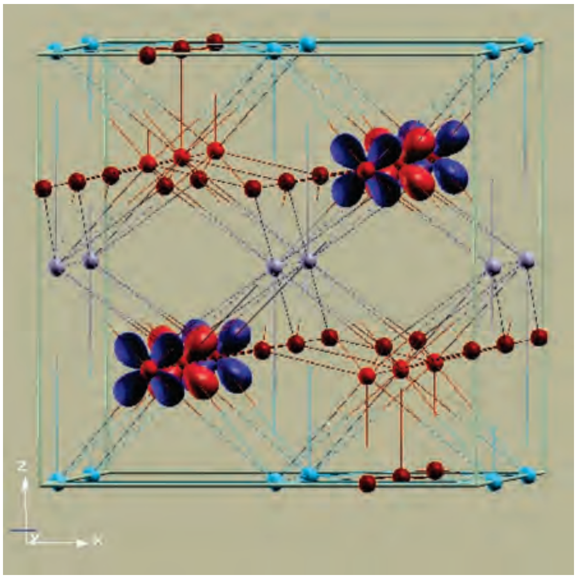

Figure 5. Spin density plot (isosurface at 0.15 e/Å^3 produced using XCRYSDEN) to illustrate the ordering of the d_{xz} orbital in the G-type ground configuration obtained by GGA+U within $U = 5.0$ eV. Red and blue denote a spin down Fe^{2+} atom and a spin up Fe^{2+} atom, respectively.

As is well-known, the Verwey charge ordering model that fulfills the so-called Anderson criterion[28] possesses the minimum electrostatic repulsion energy among all the possible charge ordering patterns. In $YBaFe_2O_5$, instead of having all Fe^{2+} and Fe^{3+} neighbors, the respective isovalent atoms arrange themselves in chains along *y* axis. Because such an arrangement is less stable elctrostatically, it must be stabilized by other mechanisms. The d_{xz} orbital ordering of the Fe^{2+} cations prefers the AFM interaction through superexchange in the *xz* plane, in combination with the AFM superexchange coupling through Fe−O p−Fe^{2+} and Fe−O p−Fe^{3+} along the *y* direction, which results in the G-type AFM state in $YBaFe_2O_5$. In addition, the charge-orbital order pattern (the alternating Fe^{2+} and Fe^{3+} cations along the *x* and *z* directions) makes the lattice stress less pronounced and reduces its contribution to the total energy. Therefore, we propose that the competition of these three (electrostatic, elastic, and magnetic) contributions to the total energy appear to be responsible for the charge order, which is realized in the experimentally observed low-temperature orthorhombic structure. In addition, this scenario may also switch on in

---

(24) Leonov, I.; Yaresko, A. N.; Antonov, V. N.; Korotin, M. A.; Anisimov, V. I. *Phys. Rev. Lett.* **2004**, *93*, 146404.

(25) Leonov, I.; Yaresko, A. N.; Antonov, V. N.; Schwingenschlögl, U.; Eyert, V.; Anisimov, V. I. *J. Phys.: Condens. Matter* **2006**, *18*, 10955.

(26) García, J.; Subías, G. *J. Phys.: Condens. Matter* **2004**, *16*, R145.

(27) Angst, M.; Khalifah, P.; Hermann, R. P.; Xiang, H. J.; Whangbo, M. H.; Varadarajan, V.; Brill, J. W.; Sales, B. C.; Mandrus, D. *Phys. Rev. Lett.* **2007**, *99*, 086403.

(28) Anderson, P. W. *Phys. Rev.* **1956**, *102*, 1008.

the framework of $YBaCo_2O_5$. On the other hand, the charge-ordered arrangement of the di and trivalent ions in $YBaMn_2O_5$ has all alivalent neighbors. The $d_{x^2-y^2}$ orbital ordering for Mn^{3+} ions favors the AFM superexchange coupling in *xy* plane through the bridged oxygen, because of the variation of the $Mn^{2+}-O-Mn^{3+}$ from the ideal 180°. The $d_{x^2-y^2}$ orbital ordering is responsible for the stability of the G-type AFM spin ordering and the charge ordering pattern which fulfills the Anderson condition. We therefore arrive at the intriguing conclusion that the orbital ordering, charge ordering, and spin ordering intimately interact, compete, and lead to the ground-state with various charge-orbital-spin ordering patterns in different systems.

Conclusions

In summary, we have preformed systematic GGA and GGA+U calculations for the oxygen defect double perovskite transition-metal oxide $YBaFe_2O_5$. We conclude that $YBaFe_2O_5$ is an insulator with an energy band gap of 1.20 eV. Because the screening of the e_g orbitals is so effective, the total charge disproportion and the derivation of the magnetic moments is rather small. The charge order is clearly indicated from the difference between the t_{2g} orbital occupation between Fe^{2+} and Fe^{3+} atoms. The obtained charge ordering arrangement violates the so-called Anderson criterion. Moreover, the analysis of spin density plot and DOS inevitably demonstrates the d_{xz} orbital ordering of Fe^{2+} cations. The orbital ordering corresponds to the local distortions of the oxygen square-pyramidal coordination. In addition, the d_{xz} orbital ordering is responsible for the stability of the G-type AFM spin ordering and the charge ordering pattern.

Acknowledgment. The authors wish to express thanks to F. M. Gao for fruitful discussions and critical reading of the manuscript, and also thank Dr. P. Blaha and V. Pardo for their help with XcrySDen applications. This work was supported by the National Natural Science Foundation of China (Grants 20331030, 20671088, 20661026, 20571073, and 20771100).

IC800060C